Journal of Applied Polymer Science

Enhancing water swelling ability and mechanical properties of water-swellable rubber by PAA/SBS nanofiber mats

Nazila Dehbari,[1] Javad Tavakoli,[2] Jinchao Zhao,[3] Youhong Tang[1]

[1]Centre for NanoScale Science & Technology and School of Computer Science, Engineering and Mathematics, Flinders University, Bedford Park, SA 5042, Australia

[2]Medical Device Research Institute (MDRI) and School of Computer Science, Engineering & Mathematics, Flinders University, Bedford Park, SA 5042, Australia

[3]School of Chemistry and Chemical Engineering, Hubei Biomass Fibres and Eco-Dyeing & Finishing Key Laboratory, Wuhan Textile University, Wuhan 430064, People's Republic of China

Correspondence to: J. Zhao (E-mail: jczhao@wtu.edu.cn); and Y. Tang (E-mail: youhong.tang@flinders.edu.au)

ABSTRACT: Investigation of the potential use of nanofibers to reinforce composites has gained significance in many applications. In this article, the nanofiber mats of poly(acrylic acid) (PAA) and styrene–butadiene–styrene (SBS) triblock copolymer with composites structure were interweaved by double needle electrospinning process. The multiple nanofiber mats were added to conventional water-swellable rubber (WSR). Improved mechanical and physical properties of WSR were obtained. Enhancement of the swellability of WSR + PAA/SBS nanofiber mats was derived from the PAA constituent absorbing water from the surface into the bulk and introducing random internal water channels between discontinuous superabsorbent polymers. The role of SBS nanofibers in the composite of WSR + PAA/SBS nanofiber mats was more related to the mechanical properties, where the breaking force of the composite increased to twice that of the conventional WSR. Interestingly, after immersion of the WSR + PAA/SBS nanofiber mats in water for 1 week, there was only a slight decrease in their mechanical properties of less than 5% compared to the dry state. The mechanisms and effects of the nanofiber mats in enhancing the mechanical and water swelling properties of WSR are also discussed. © 2016 Wiley Periodicals, Inc. J. Appl. Polym. Sci. **2016**, *133*, 44213.

KEYWORDS: electrospinning of nanofibers; mechanical properties; water channel; water swellable rubber

Received 9 May 2016; accepted 21 July 2016
DOI: 10.1002/app.44213

INTRODUCTION

Water-swellable rubbers (WSRs) are consisted of rubber parts with high resilience, elasticity, toughness, and stretch-ability and water absorption parts with super water absorption ability.[1,2] In terms of their ability to absorb and retain water, these new materials are generally used for sealing applications in constructions, subways, and subsea tunnels, as well as aircraft apparatus. They also can be used in the food, agricultural, and horticultural industries, as well as medical usage such as sanitary products, medicine and drug delivery systems.[3–7] WSRs are normally prepared by multicomponent blending of a rubber matrix, superabsorbent polymers (SAPs) and other hydrophilic/hydrophobic fillers through physical mixing or chemical surface grafting. Chemical methods are less environmentally friendly, more complicated and expensive than other methods.[2,8–11]

The poor mechanical property of WSRs after swelling is the major problem that limits their applications. Aggregation of SAP particles forming discontinuous phases, as well as poor interfacial properties and nonhomogeneous dispersion, often leads to remarkably poor mechanical properties, instability of water-swelling characterization, and short-term water retention.[1,9,12,13] Therefore, to promote mechanical properties, the miscibility of SAP and rubber needs to be improved. The introduction of a compatibilizer is one of the immediately effective methods to enhance the dispersion of two immiscible components that can react with both hydrophobic rubber matrix and hydrophilic SAPs.[14] In our previous research, it was shown that using (3-aminopropyl)-triethoxysilane as a compatibilizer had a marked impact on the physical properties of WSR composites.[15] However, SAPs trapped within the rubber matrix remained isolated. In further experiments, we observed that poly(acrylic acid) (PAA) nanofibers in WSR composites could produce feasible connections known as water channels between SAPs,[16] thereby transferring water between SAPs efficiently. Furthermore, the introduction of nanofibers/mats into WSR composites has led to significant improvement in the mechanical properties of WSR,

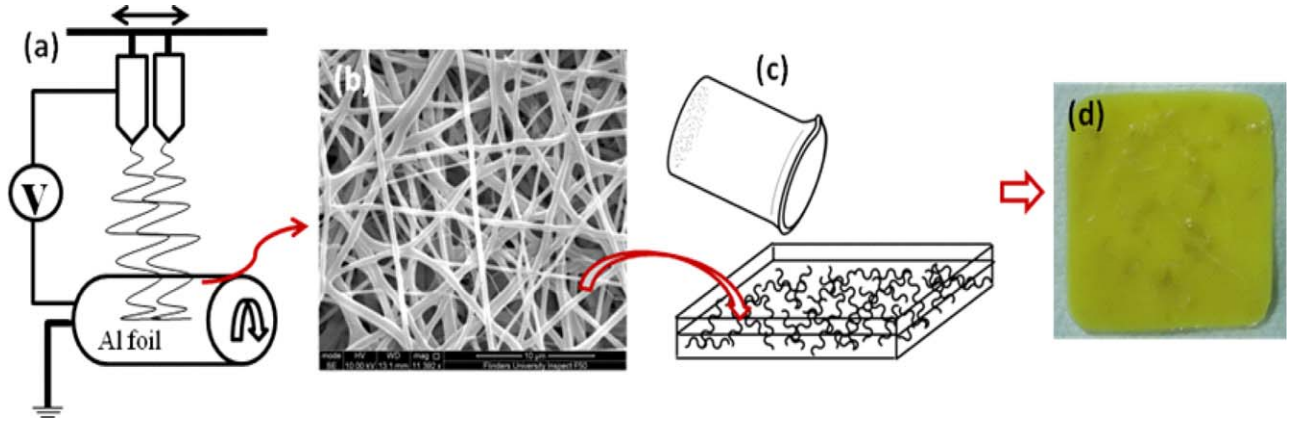

Scheme 1. Steps of preparation of WSR enhanced with PAA/SBS nanofiber mats (a) the electrospinning machine with a setting of two needles; (b) SEM image of the PAA/SBS nanofibers; (c) mixing of PAA/SBS nanofibers with WSR; and (d) the cured composite of WSR + PAA/SBS nanofibers. [Color figure can be viewed in the online issue, which is available at wileyonlinelibrary.com.]

depending on the type of nanofiber.[17–20] For example, highly elastic styrene–butadiene–styrene (SBS) nanofibers with high tensile strength are known to be an effective choice for enhancement of the mechanical properties of WSR.[21–24] It seems that the hydrophobic properties of rubber matrix and SBS nanofibers lead to miscibility of the constituents of appropriate composites and result in better stress distribution.

In this article, the contributions of SBS and PAA nanofibers produced by double needle electrospinning method to improvement of the mechanical and swelling properties of WSR composites were investigated. The aim of this study was twofold: first, to understand how the mechanical properties of WSR may be changed by introducing different types of nanofiber (PAA, SBS, and PAA/SBS) and, second, investigation of the role of the nanofibers in the swelling properties of WSR composites.

EXPERIMENTAL

Materials

PAA particles (average $M_w \sim 450{,}000$ g/mol), PAA solution (average $M_w \sim 250{,}000$ g/mol), ethylene glycol (EG) (anhydrous, 99.8%), sulfuric acid, dimethylformamide (DMF), tetrahydrofuran (THF), and (3-aminopropyl)-triethoxysilane used as a compatibilizer were purchased from Sigma Aldrich, Australia. SBS triblock copolymer was supplied by Yueyang Bailing Huaxing Chemicals Co., Ltd. (Yueyang, China) (average $M_w \sim 300{,}000$ g/mol), and banana skin silicone rubber was purchased from Barnes Products Pty Ltd. (Australia). All chemicals were used without purification. All aqueous solutions were prepared using Milli-Q water at 25 °C.

Sample Preparation

The PAA solution was prepared according to previous work.[25,26] Briefly, 0.96 g EG was added to 100 g 6 wt % PAA/ethanol solutions as a crosslinking agent with the concentration of 16 wt % relative to the PAA. A homogeneous solution was obtained by gentle mechanical stirring at room temperature. Prior to electrospinning, sulfuric acid (1 mol/L) was added to the PAA solution at a concentration of 50 μL/mL. For the SBS solution, 12 g of SBS was dissolved in a mixed solution of 13.67 g DMF and 41 g of THF with stirring. Solution electrospinning was performed by fully automatic equipment (TL01; NaBond Technologies, Shenzhen, China) consisting of a syringe-flat tip needle and a high voltage supply. To obtain optimal nanofibers without beads, the PAA and SBS solutions were electrospun with two needles at the voltage of 15 kV, feeding rate of 1.5 mL/h on an aluminium foil covered cylindrical collector with a tip-to-collector distance of 10 cm. The *x*-axis moving speed of the needle and the drum speed were set at 3.5 mm/s and 200 rpm, respectively. The whole electrospinning process lasted for about 2 h for both solutions.

The PAA and SBS nanofibers obtained were used in the WSR composites to strengthen their physical and mechanical properties. The composites were prepared through a solution impregnation technique as shown in Scheme 1. In detail, 12.5 g PAA was mixed with 2.0 g EG (cross-linking agent), 0.625 g sulfuric acid (dehydration agent), and 0.0625 g (3-aminopropyl)-triethoxysilane (compatibilizer) before being added to 20.0 g of part A of the rubber. The final mixture was prepared by adding 20.0 g of part B of the rubber to the solution while stirring for 10 min before moulding. Prepared PAA, SBS, and PAA/SBS nanofibers with thickness of 0.04 mm with different ratios cut into 0.5×5 cm^2 strips were added to the final solution. The ratio of PAA nanofibers was kept constant at 1 wt % in all composites to investigate the role of SBS nanofibers within the composites and the water-swellability of the composites, i.e., 1 wt % PAA nanofiber and 2 wt % PAA/SBS nanofiber, respectively. Following 24 h of curing at ambient temperature, WSR composites consisting of PAA, SBS, and PAA/SBS nanofiber were obtained. For the control experiment, conventional WSR composite was prepared under the same conditions.

Characterization

The surface morphology and distribution of the electrospun PAA and SBS nanofibers in all composite samples before and after swelling were characterized using scanning electron microscopy (Inspect F50; FEI, Oregon, USA). Prior to using SEM, a K575X sputter coater was used for deposition of a very thin platinum film (~2 nm) on the surfaces of all samples. The average diameter of nanofibers obtained from SEM was measured by the Image software, and the diameters of nanofibers within the composite before and after swelling were compared

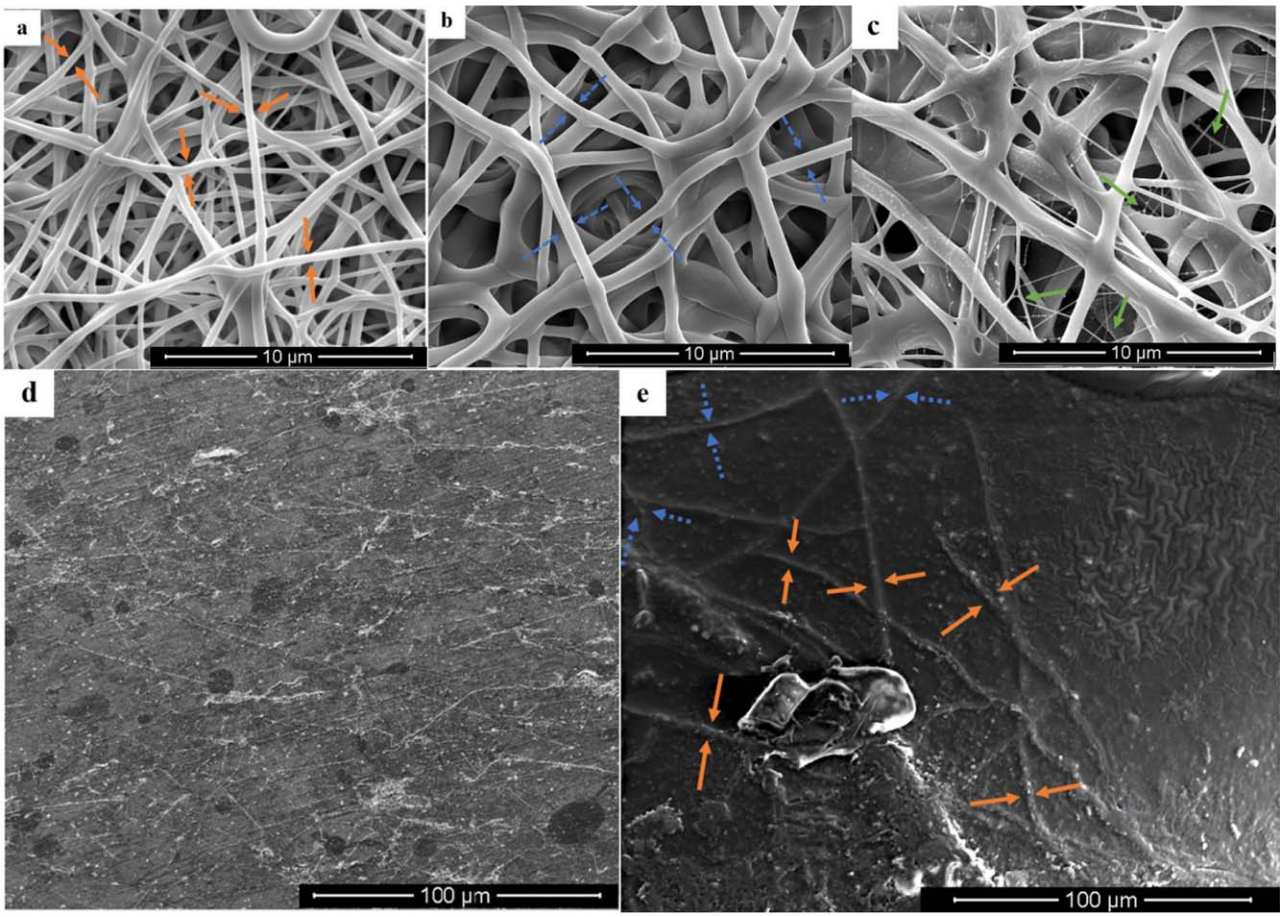

Figure 1. SEM micrographs of (a) PAA nanofibers with average diameter of 0.65 μm (solid orange arrows), (b) SBS nanofibers with average diameter of 0.95 μm (dashed blue arrows), (c) PAA/SBS nanofibers with some spiderweb-like structures (solid green arrows), and WSR + PAA/SBS composites (d) before and (e) after swelling, the bold channels representing PAA nanofibers that have absorbed water (solid orange arrows). [Color figure can be viewed in the online issue, which is available at wileyonlinelibrary.com.]

for further investigation. Surface wettability, surface tension, and contact angle measurements of nanofibers and all composites were carried out with a Sinterface machine. The mechanical properties of nanofibers and composites, namely elongation at breaking point, ultimate strength, and extensibility before and after immersion in water were measured by an Instron materials testing machine (Instron, USA). All reported mechanical results represent average values from three samples with the same dimensions. The force–stretch curves are reported due to the large deformation occurring in the samples. The swelling behaviours of WSR composites were tested by measuring the initial weight of the dry samples (m_0) and subsequently after they had been immersed in Milli-Q water (500 mL) at 25 °C from 1 h to several days. The swollen sample was then weighed at regular intervals (m_1). Before measurement of the weight of the swollen samples, the excess surface water was removed by filter paper. The swelling ratio was calculated using the following equation:

$$\frac{m_1 - m_0}{m_0} \times 100 \quad (1)$$

To investigate the effect of PAA nanofibers within the WSR matrix, a repeated swelling test was also performed. Each sample was dried at 70 °C until it achieved a constant weight. Then, the samples were again immersed in water at room temperature. After a specified time, they were taken out and the excess moisture on the surface was removed. The swelling ratio was calculated using the following equation:

$$\frac{m_3 - m_2}{m_2} \times 100 \quad (2)$$

where m_2 and m_3 are the weights of a sample before and after the second water swelling, respectively. To ensure that ultrafine PAA nanofibers remained in the composites after the swelling experiment, all samples were dried, weighed, and compared with their initial weight.

RESULTS AND DISCUSSION

Morphology

SEM images of PAA, SBS, and PAA/SBS nanofiber mats and WSR including PAA/SBS nanofibers (WSR + PAA/SBS) before and after swelling are shown in Figure 1. The average diameter of PAA and SBS is about 0.65 and 0.96 μm, respectively (Figure 1a and b). The image of the PAA/SBS nanofiber mat (Figure 1c) indicates that an interlinked structure composed of SBS and PAA nanofiber mats was prepared. The use of doubleneedle electrospinning was effective for creating an entangled network

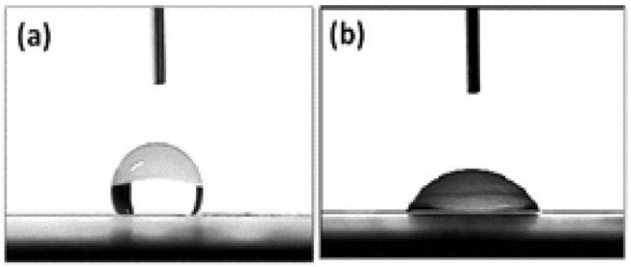

Figure 2. Contact angle images of (a) SBS nanofiber mat and (b) PAA/SBS nanofiber mat 30 s after a drop of water was put on the surface.

consisting of two different types of fiber with sizes ranging from submicron to nanometer. Arrangement of these fibers resulted in the formation of a spiderweb-like structure[27–29] that increased the hydrophilicity and specific surface area while also affecting porosity.[16] Figure 1d shows a WSR composite with randomly distributed PAA/SBS nanofibers in the dry state. After immersion in water, PAA nanofibers showed a slight increase in diameter (0.93 μm in average) and an increase in their tendency to take up water. Unsurprisingly, the size of SBS nanofibers that were embedded in rubber matrix remained unchanged form that of SBS nanofibers in the dry state.

Contact Angle of Nanofiber Mats

As was shown in Figure 2, the surface hydrophilicity of the SBS nanofiber mat (Figure 2a) is very different from that of the PAA/SBS nanofiber mat (Figure 2b). A significant decrease in contact angle in the PAA/SBS nanofiber mat, from 117° in Figure 2a to 73° in Figure 2b after a drop of water has been put on the surface for 30 s, indicates that the addition of PAA nanofibers to SBS nanofibers increased surface hydrophilicity. Therefore, enhancement of the hydrophilicity of SBS nanofibers may change the bulk properties while increasing the water uptake capability of the WSR + PAA/SBS composite.

Mechanical Properties of Nanofiber Mats and Composites

Figure 3 shows the mechanical behaviors of PAA, SBS, and PAA/SBS nanofibers in the dry state. The average elongation as well as average force at the breaking point are significantly enhanced in the PAA/SBS nanofiber mats in comparison with the PAA nanofiber

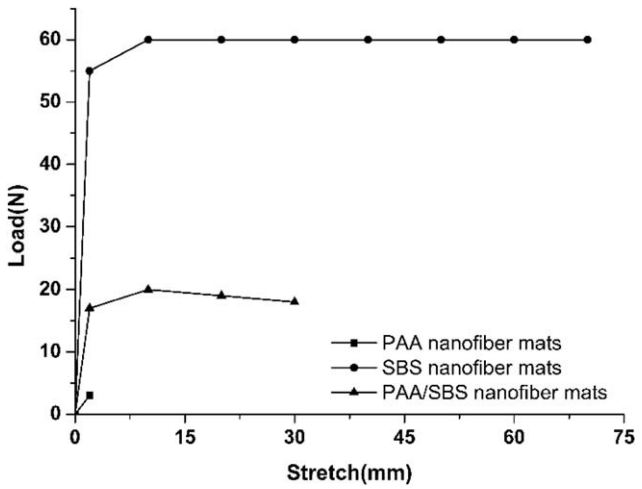

Figure 3. Force-stretch curves of PAA, SBS, and PAA/SBS nanofiber mats.

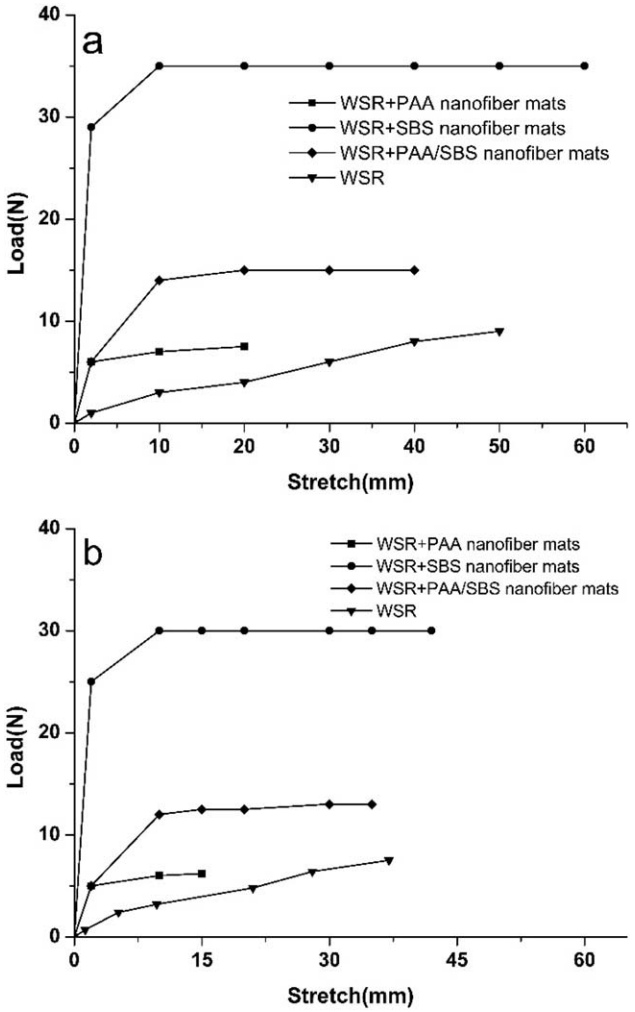

Figure 4. Force–stretch curves of composites with PAA, SBS, and PAA/SBS nanofibers (a) before and (b) after immersion in water.

mats. The mechanical contribution of super-elastic SBS nanofibers to the brittle PAA nanofiber structure—shown in SEM images to be like spiderweb networks with mechanical interlocking between two types of nanofibers—resulted in a better distribution of stress across the mats. This led to 15 and 7 times greater stretchability and breaking force for SBS/PAA nanofiber mats, compared to the values found for PAA nanofiber mats, respectively.

Figure 4 shows the force–stretch curves of composites with PAA, SBS, and PAA/SBS nanofiber mats before and after immersion in water for 1 week. A similar trend for WSR+PAA, WSR + SBS and WSR+PAA/SBS nanofiber composites was observed when compared to the trends of the nanofibers alone. In Figure 4a, it can be seen that the breaking force of WSR with PAA nanofibers at the specific elongation of 20 mm increases from 4.0 *N* (for the conventional WSR composite) to 7.5 *N*. With the introduction of PAA nanofibers into WSR, however, the elongation at break decreases from 50 to 20 mm. The addition of SBS nanofiber mats to the WSR composite enhances the mechanical properties markedly from those in the dry state. Both force and elongation to break for WSR + SBS composite reaches the maximum value, i.e., 35 *N* and 60 mm. However, the WSR + SBS composite does not

Table I. Mechanical Properties of PAA, SBS, and PAA/SBS Reinforced WSR Composites before and after Swelling

	WSR + PAA nanofiber	WSR + SBS nanofiber	WSR + PAA/SBS nanofiber
Before swelling			
Elongation at break (mm)	20	60	40
Breaking force (N)	7.5	35	15
After swelling			
Elongation at break (mm)	15	44	37
Breaking force (N)	5.8	30	13

display enhanced water-swellable ability, due to the hydrophobic characteristic of SBS. For the WSR + PAA/SBS nanofiber composite, the breaking force was twice as high as that of WSR alone, with a slight decrease in stretchability.

Figure 4b shows the mechanical properties of WSR with PAA, SBS, and PAA/SBS nanofiber mats after immersion in water for 1 week. The swelling has an adverse effect on the mechanical properties of the WSR composites, as the elongation and force at breaking point decrease for all samples in comparison to the dry state. The mechanical properties of WSR + PAA nanofiber mats and WSR + SBS nanofiber mats decrease by about 20–30% after swelling; however, the introduction of PAA/SBS nanofiber mats into the WSR limits the decrease to less than 5%. Table I gives the mechanical properties of the PAA, SBS, and PAA/SBS reinforced WSR composites before and after swelling.

Swelling Ratio of Composites

The water absorption properties of samples for the first and second swellings in water are shown in Figures 5 and 6. As can be seen, the initial swelling ratio of all composites for both first and second immersions in water is very high. In the latter stage,

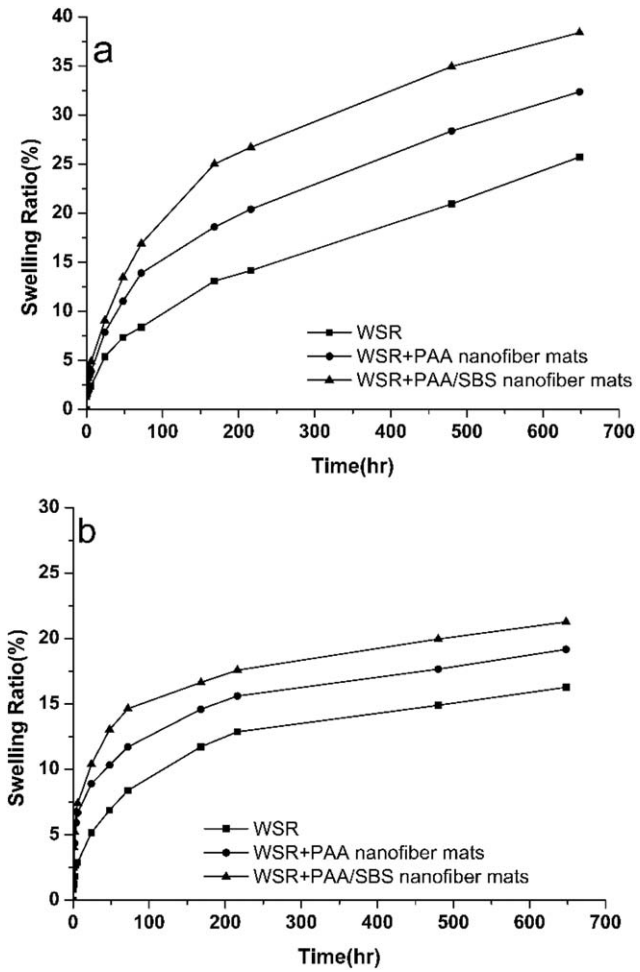

Figure 5. Water absorption ability of composites in (a) first and (b) second swellings to 650 h.

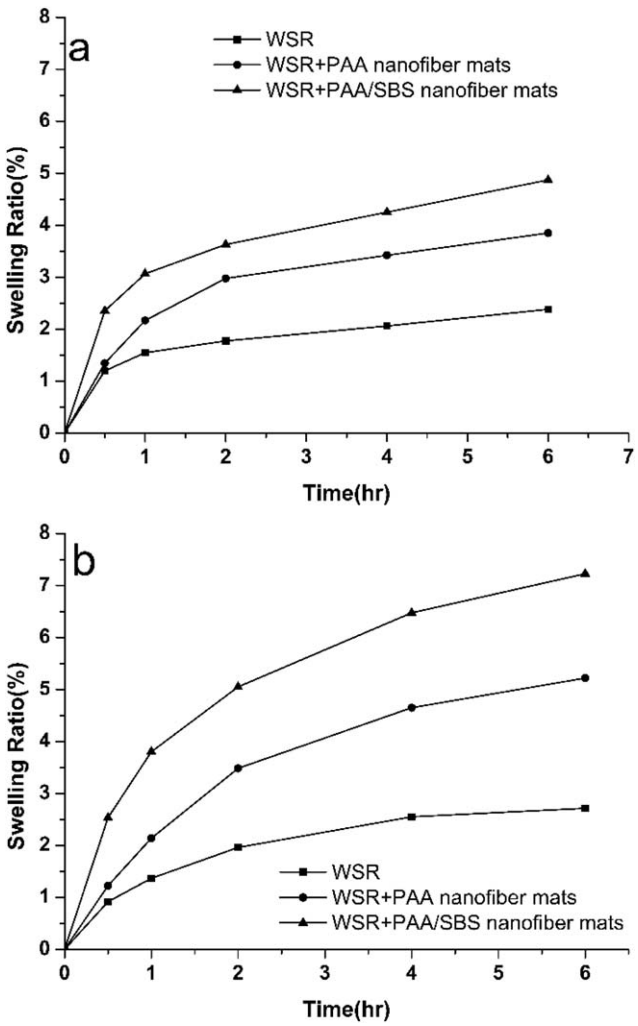

Figure 6. Water absorption ability of composites at (a) first and (b) second absorption periods for the first 6 h.

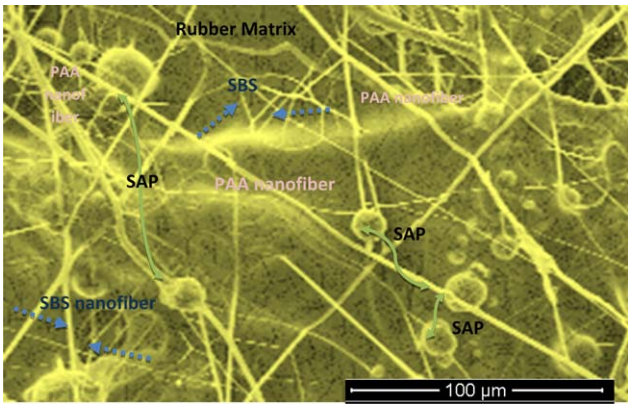

Figure 7. SEM images showing the proposed mechanism of WSR containing PAA and SBS nanofiber mats after the swelling state (dashed blue arrows point to SBS nanofibers). [Color figure can be viewed in the online issue, which is available at wileyonlinelibrary.com.]

the increase in the swelling ratio as a function of time becomes slower than that in the initial stage.[30,31] However, the composites did not reach an equilibrium state after 650 h for both first and second immersion in water, as shown in Figure 5.

The swelling properties of WSR improved with the incorporation of PAA and PAA/SBS nanofiber mats into the WSR (Figure 5a). The PAA constituent of PAA/SBS nanofiber mats played an important role in absorbing water from the surface into the bulk by introducing water channels in the WSR composite and linking discontinuous PAA particles. This is consistent with our previous results.[16] As reported in Figure 5b, all samples exhibit a lower swelling ratio in second swelling after 650 h; however, the WSR + PAA/SBS nanofiber mats composite experiences a higher swelling ratio (about 40%) in the initial stage of swelling (first 6 h) than that in the second swelling stage in comparison with that for the first swelling, as shown in Figure 6. The introduction of SBS/PAA nanofiber mats into the WSR had a marked effect on the second swelling at nanolevel by increasing the hydrophilicity of the bulk and surface of the WSRs. The conventional WSR showed the same trend and amount of swelling ratio in both the first and second swelling tests, but with the introduction of PAA/SBS nanofiber mats into the WSR, the water absorption rate in the initial stage was enhanced, especially in the repeated swelling periods.

Mechanisms of Enhanced Swelling Ratio and Mechanical Properties

The mechanical properties and swelling ratio of the WSR composites were significantly enhanced by the introduction of PAA/SBS nanofiber mats. Figure 7 depicts the proposed mechanism of nanofibers within the rubber after immersion in water, which was observed by SEM. The PAA and SBS nanofibers in the PAA/SBS nanofiber mats entangled mechanically with each other to provide a spiderweb network within the matrix. These networks could act as the internal reinforcements to enhance the mechanical properties of WSR (similar to the enhancement in fibre-reinforced composites) even after the water absorption. Meanwhile, during the early stage of swelling those networks could induce water into the rubber more quickly and make random interconnections among discontinuous SAP particles. Therefore, the transfer of water from the surface to the bulk of the composite and between isolated SAPs trapped by the rubber matrix could occur more quickly than in conventional WSR, as shown in Figure 1e. As a result, excellent water swelling ability and mechanical properties were achieved.

CONCLUSIONS

In this study, electrospun nanofibers of PAA, SBS, and PAA/SBS were prepared by the electrospinning method. The resultant nanofibers were introduced to enhance the mechanical properties and water swellability of conventional WSR. In SEM images of PAA/SBS nanofiber mats, some spiderweb networks were observed with physical entanglements between nanofibers of PAA and SBS. The PAA constituent of PAA/SBS nanofiber mats could enhance the water absorption of the composite, while the mechanical properties of the WSR composite were improved by SBS nanofiber mats. The proposed mechanism was illustrated.

ACKNOWLEDGMENTS

Y. Tang is grateful for the support of the Australian Research Council with a Discovery Early Career Research Award Grant (DE120102784) for the research work. J. Zhao is grateful for the support of National Natural Science Foundation of China (no. 51303138).

REFERENCES

1. Nakason, C.; Nakaramontri, Y.; Kaesaman, A.; Kangwansukpamonkon, W.; Kiatkamjornwong, S. *Eur. Polym. J.* **2013**, *49*, 1098.
2. Wang, G. J.; Li, M.; Chen, X. F. *J. Appl. Polym. Sci.* **1999**, *72*, 577.
3. Wu, J.; Lin, J.; Li, G.; Wei, C. *Polym. Int.* **2001**, *50*, 1050.
4. Mignon, A.; Graulus, G.; Snoeck, D.; Martins, J.; De Belie, N.; Dubruel, P.; van Vlierberghe, S. *J. Mater. Sci.* **2015**, *50*, 970.
5. Yamashita, S.; Kodama, K.; Ikeda, Y.; Kohjiya, S. *J. Polym. Sci. A: Polym. Chem.* **1993**, *31*, 2437.
6. Saijun, D.; Nakason, C.; Kaesaman, A.; Klinpituksa, P. *Songklanakarin J. Sci. Technol.* **2009**, *31*, 561.
7. Qian, M.; Hua, F. *J. Mater. Sci.* **2001**, *36*, 731.
8. Gong, J. P.; Katsuyama, Y.; Kurokawa, T.; Osada, Y. *Adv. Mater.* **2003**, *15*, 1155.
9. Zhang, Z. H.; Zhang, G.; Li, D. F.; Liu, Z. C.; Chen, X. F. *J. Appl. Polym. Sci.* **1999**, *74*, 3145.
10. Meng, E.; Zhang, X.; Benard, W. In MEMS Materials and Processes Handbook; Ghodssi, R.; Lin, P., Eds.; Springer: New York, **2011**; p 193.
11. Amnuaypanich, S.; Patthana, J.; Phinyocheep, P. *Chem. Eng. Sci.* **2009**, *64*, 4908.
12. Magalhães, A. S. G.; Neto, M. P. A.; Bezerra, M. N.; Ricardo, N. M. P. S.; Feitosa, J. P. A. *Quim. Nova* **2012**, *35*, 1464.

13. Wang, C.; Zhang, G.; Dong, Y.; Chen, X.; Tan, H. *J. Appl. Polym. Sci.* **2002**, *86*, 3120.
14. Utracki, L. A. *Can. J. Chem. Eng.* **2002**, *80*, 1008.
15. Dehbari, N.; Zhao, J.; Peng, R.; Tang, Y. *J. Mater. Sci.* **2015**, *50*, 5157.
16. Zhao, J.; Dehbari, N.; Han, W.; Huang, L.; Tang, Y. *Mater. Des.* **2015**, *86*, 14.
17. Chen, C. H.; Cheng, S. *Compos. Mater.* **1967**, *1*, 30.
18. Mallick, P. K. Book Review: Fiber-Reinforced Composites: Materials, Manufacturing, and Design; Marcel Dekker, Inc.: New York, **1988**; p 469.
19. Huang, Z. M.; Zhang, Y. Z.; Kotaki, M.; Ramakrishna, S. *Compos. Sci. Technol.* **2003**, *63*, 2223.
20. Coleman, J. N.; Khan, U.; Blau, W. J.; Gun'ko, Y. K. *Carbon* **2006**, *44*, 1624.
21. Subbiah, T.; Bhat, G. S.; Tock, R. W.; Parameswaran, S.; Ramkumar, S. S. *J. Appl. Polym. Sci.* **2005**, *96*, 557.
22. Kim, J. S.; Reneker, D. H. *Polym. Compos.* **1999**, *20*, 124.
23. Park, M.; Im, J.; Shin, M.; Min, Y.; Park, J.; Cho, H.; Park, S.; Shim, M. B.; Jeon, S.; Chung, D. Y.; Bae, J.; Park, J.; Jeong, U.; Kim, K. *Nat. Nanotechnol.* **2012**, *7*, 803.
24. Borba, P.; Tedesco, A.; Lenz, D. *Mater. Res.* **2014**, *17*, 412.
25. Ding, B.; Li, C. R.; Miyauchi, Y.; Kuwaki, O.; Shiratori, S. *Nanotechnology* **2006**, *17*, 3685.
26. Meng, L.; Klinkajon, W.; K-hasuwan, P.; Harkin, S.; Supaphol, P.; Wnek, G. E. *Polym. Int.* **2015**, *64*, 42.
27. Wang, X.; Ding, B.; Sun, G.; Wang, M.; Yu, J. *Prog. Mater. Sci.* **2013**, *58*, 1173.
28. Pant, H. R.; Bajgai, M. P.; Nam, K. T.; Seo, Y. A.; Pandeya, D. R.; Hong, S. T.; Kim, H. Y. *J. Hazard. Mater.* **2011**, *185*, 124.
29. Heikkilä, P.; Harlin, A. *Eur. Polym. J.* **2008**, *44*, 3067.
30. Zhang, Z. H.; Zhang, G.; Zhang, Y.; Wang, Z. G.; Yu, D. H.; Hu, X. Q.; Hu, C. Q.; Tang, X. Y. *Polym. Eng. Sci.* **2004**, *44*, 72.
31. Zhang, Y. H.; He, P. X.; Zou, Q. C.; He, B. Q. *J. Appl. Polym. Sci.* **2004**, *93*, 1719.